

Comments of referee #3.

1. The authors state that their work was partially inspired by the work of Schmitt and Heymsfield 2010. While there are substantial similarities in some of the particle probe simulations, the work by Schmitt and Heymsfield did not use any remote sensing data. The authors of this work state that Schmitt and Heymsfield used remote sensing data from ARM to constrain the relationship between alpha and beta. The ARM data presented were another aircraft particle probe dataset. The authors should re-read the right column on page 1612 of Schmitt and Heymsfield to understand how the alpha factor was mathematically (not empirically) determined in that study.

“Schmitt and Heymsfield (2010, hereafter SH2010) have simulated the aggregation of plates and columns. Fractal 2D and 3D analyses calculated from the box counting method (Tang and Marangoni 2006) stated that the fractal coefficient in the 3D space is equal to β . This allowed to derive a relationship that calculates the exponent β from the 2D fractal dimension of the 2D images. Once β has been fixed, the pre-factor α is calculated from the area measurement.”

I would also encourage the authors to try this method and see how it compares to their alpha values.

In our study presented, it is not stated that β is equal to the fractal dimension in the 3D space. Of course, we would be interested working with the authors of SH2010 to make a separate study on the comparison of our 2 methods. The comparison is beyond the scope of this study.

2. The authors state that they only used the 2DS probe for area dimensional relationships even though PIP data was available. How much difference was there between 2DS and PIP area measurements at the largest sizes that the 2DS was seeing? There will obviously be discrepancies at small (for the PIP) sizes, but there shouldn't be too much difference at larger sizes (more than 20 pixels for the PIP).

In general, differences between the mean projected surface from 2DS images and from PIP images within the overlapping size range do not show large discrepancies (figure 1).

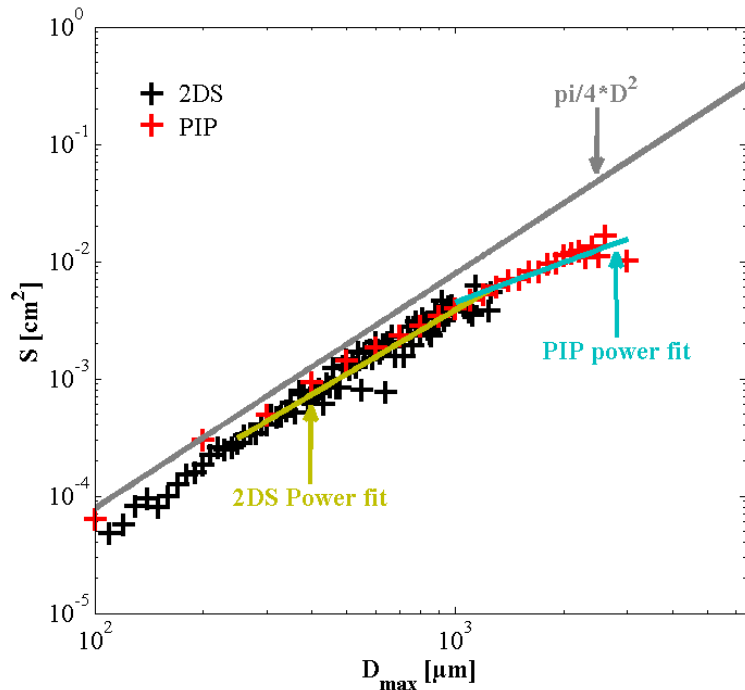


Figure 1 : Mean projected surface in cm² on y-axis versus D_{max} in μm on the x-axis. Black symbols represent the 2DS image data and red symbols the PIP data. The grey line would be the power law fit for spherical particles. The golden line is the power law which fits the 2DS data for D_{max} larger than 250μm and the blue line fits the PIP data with a power law for D_{max} larger than 950μm.

My concern is that in not using the PIP area information for the largest sizes, you may be losing valuable information on the fractal properties of the particle population. The density values determined

for large particles suggest that there should be a lot of graupels or hail present, and it is likely that the PIP would show that better.

See also our detailed answer on similar referee #1 comments.

Shortly, we now introduced a 2D-S plus PIP common σ exponent taking into account the 2DS and PIP 2D images. This σ exponent is calculated by weighting the two σ that are derived separately for 2D-S and PIP images, respectively, with the ratio of the surface covering the size range where each (for 2D-S and for PIP) S-D relationship has been calculated:

$$\sigma = \frac{\sum_{D_{\max}=250\mu\text{m}}^{950\mu\text{m}} N(D_{\max}) \cdot S(D_{\max})}{\sum_{D_{\max}=250\mu\text{m}}^{6450\mu\text{m}} N(D_{\max}) \cdot S(D_{\max})} \cdot \sigma_{2DS} + \frac{\sum_{D_{\max}=950\mu\text{m}}^{6450\mu\text{m}} N(D_{\max}) \cdot S(D_{\max})}{\sum_{D_{\max}=250\mu\text{m}}^{6450\mu\text{m}} N(D_{\max}) \cdot S(D_{\max})} \cdot \sigma_{PIP}$$

Also note, that aircraft probe data at large particle sizes aren't necessarily randomly oriented. This could affect your results as well. Larger particles are naturally oriented due to aerodynamic affects and this orientation may not be disturbed enough by the airflows near the probe for the orientation to be considered random.

For sure, the eventual orientation of particles during the measurement influences the resulting power laws (figure3). The fact that in our theoretical simulations, orientation is not

avored, involves that all the orientations are equally possible. However, there is no study concerning an eventual orientation of particles during their recording with cloud probes mounted on the Falcon wing stations. To quantify this uncertainty, we may take for a given calculated mass of a crystal its minimum D_{max} (which will be an underestimation with respect to its real value) and a maximum D_{max} (close to the real value) calculated with respect to the real D_{max} . By modeling both types of projected D_{max} according to the crystal mass and doing this for all simulated shapes, we obtain an uncertainty related to the projection of possibly oriented 3D hydrometeors projected on a 2D plane (figure 4).

The model error has a standard deviation of 11%, which is the error between the β calculated with the linear fit and the β calculated through the 3D simulation. For $\ln(\alpha)$ the model error has a standard deviation of 70%. By the way, this latter large error is the reason why the results obtained for pre-factors with the 3D simulations cannot be used.

Simulations of Hexagonal Columns such $L=0.2*H$

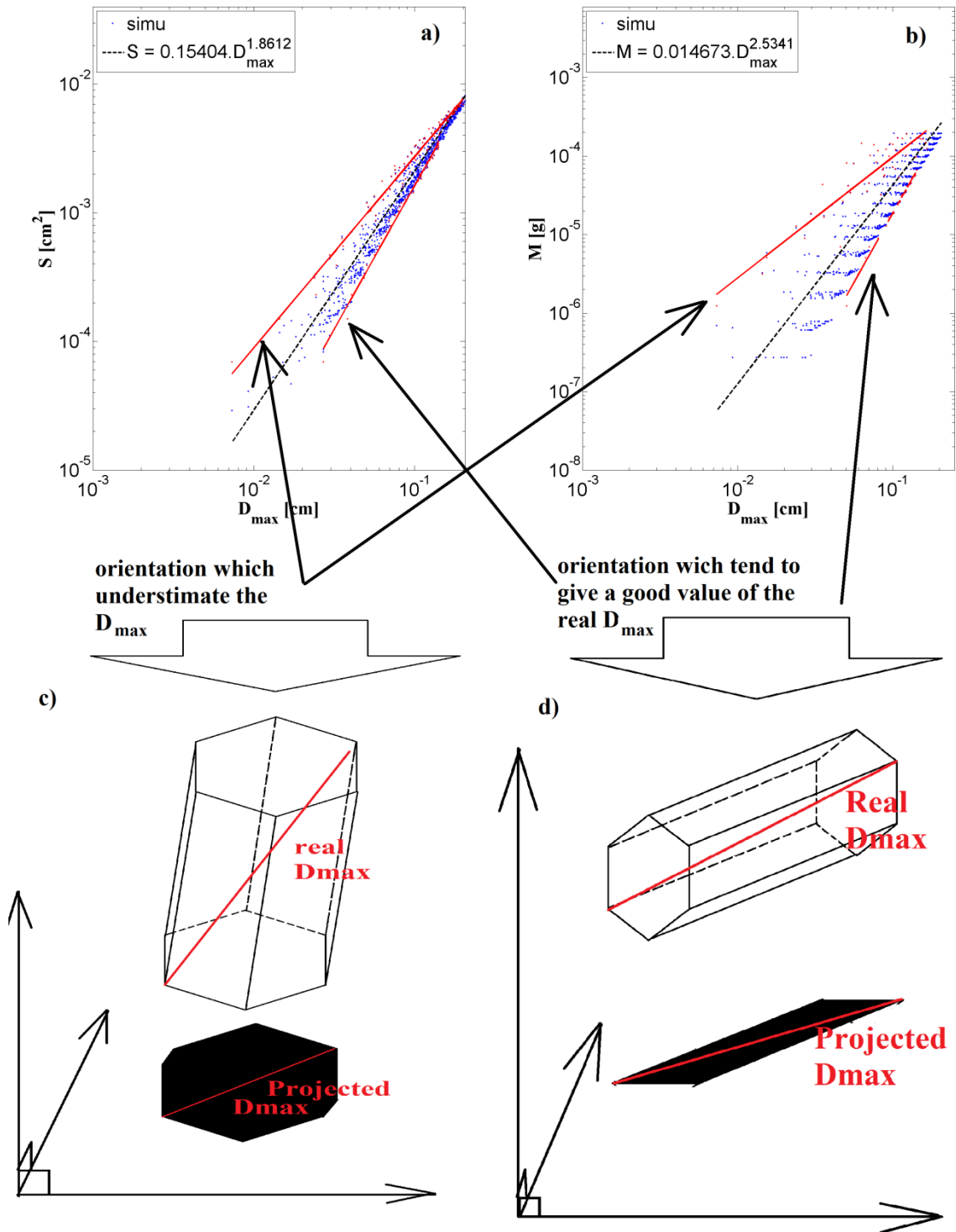


Figure 1 : Exemplary results obtained for a 3D simulation of columns characterized by Length=0.2*Height. a) $S(D)$ plot: Blue points are the simulated data for the column, red lines are power law fits enclosing most of the data points for all possible orientations. The dashed black line is the mean of the two power laws (= the mean between two red lines when the orientation underestimates D_{max} and when the orientation is close to the real D_{max}). b) $m(D)$ plot: same as for a) but with the mass of the simulated columns which is now on the y-axis; c) schematic of a 3D shape oriented in the 3D space when its orientation gives an underestimated value of the real D_{max} of the ice crystals. d) Schematic of a 3D shape oriented in the 3D space when its orientation gives a close value of the real D_{max} of the ice crystals.

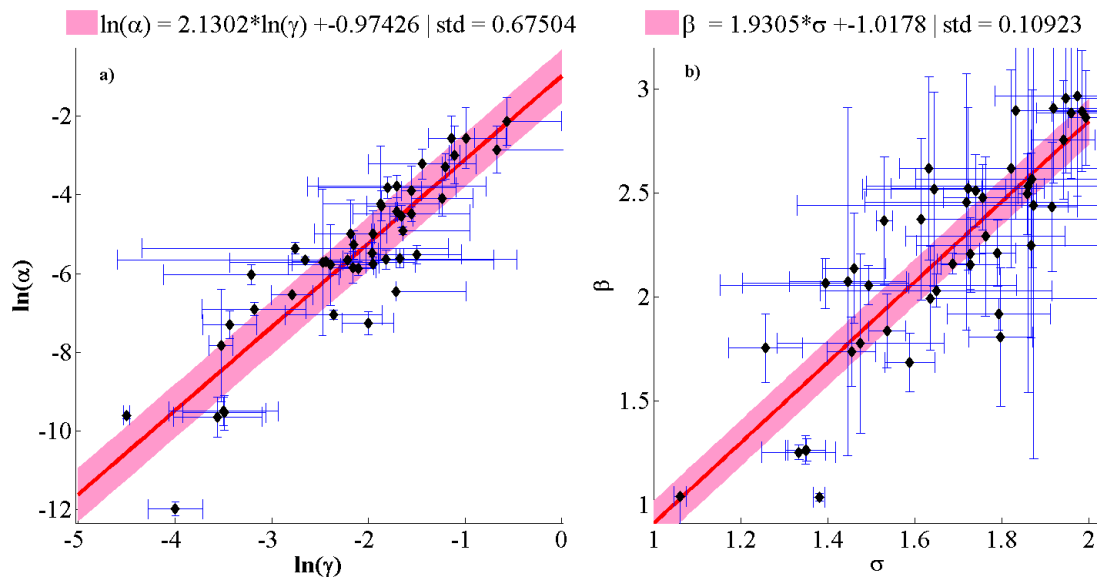


Figure 2 : Black symbols are data points for single 3D habits. Error bars give the uncertainty due to the orientation of the ice crystals during arbitrary projection on 2D plane. Red line is the linear fit between the corresponding $S(D)$ coefficients and the $m(D)$ coefficients. The pink band takes into account the standard deviation of the error between the fit and the modeled values. a) is for pre-factors and b) is for the exponents.

3. The choice of mostly pristine particle shapes for use in determining the relationship between the power is not really realistic. The shapes that you show in figure 6, how often do you see these shapes in the 2DS data or, more important, in the PIP data? This is probably part of the reason that your equation 11 is so substantially different from the results found in Schmitt and Heymsfield.

In SH2010, the study is only reported on aggregates of columns and plates. Our study wants to cover the maximum of different habits. Now, in addition and according to this reviewer's comment, additional simulations with various kinds of aggregates have been added to this study. These new simulations are also integrated to the figure 3 below. Accordingly, figure 7 of the current version of the manuscript is updated.

Table 4 is also updated to take into account the added habit types resembling aggregates and corresponding results.

Then figure 6 of the current version is updated in order to take into account reviewer#1 comments.

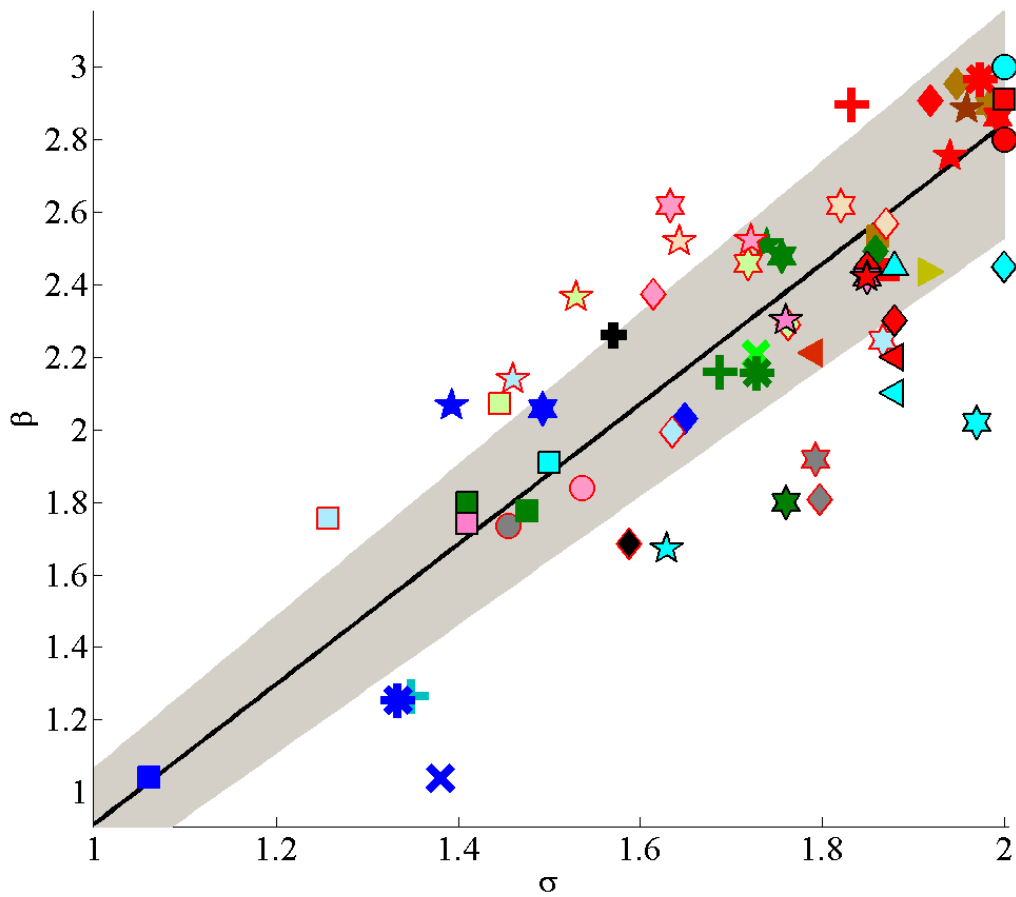



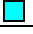

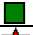






























Figure 3 : Exponent β of $m(D)$ relationships as a function of the exponent σ of the respective $S(D)$ relationships. Each data point either with red contours or without contours is deduced for a population of 1000 simulated 3D shapes and corresponding projections. Symbols with red contours are deduced for 3D aggregates of crystals of an elementary shape. Symbols with black contours stem from Mitchell (1996). The legend for symbols is given in table 4. A linear fit of all simulated data is shown by the black line. The grey band gives the mean standard deviation of 11%.

Table 1: Ice crystal types and corresponding exponents (σ) and (β) of $S(D)$ and $m(D)$ relations, respectively. The symbols in the left column are subsequently used in Fig. 8 for individual ice crystal shapes. The first part of the table stems from Mitchell (1996) where random orientation is assumed for particles with $D_{max} < 100\mu\text{m}$, whereas for particles beyond $100\mu\text{m}$ horizontal orientation is assumed. The second part of the table stems from simulations.

symbol	Description	Range	σ	β
Ice crystal shapes from Mitchell (1996)				
	hexagonal plates	$15\mu\text{m} < D_{max} < 100\mu\text{m}$	1.85	2.45
	hexagonal plates	$100 < D_{max} < 3000\mu\text{m}$	2	2.45
	hexagonal columns	$30 < D_{max} < 100\mu\text{m}$	2	2.91
	hexagonal columns	$100 < D_{max} < 300\mu\text{m}$	1.5	1.91
	hexagonal columns	$D_{max} > 300\mu\text{m}$	1.41	1.74
	rimed long columns	$200 < D_{max} < 2400\mu\text{m}$	1.41	1.8
	crystals with sector-like branches (P1b)	$10 < D_{max} < 40\mu\text{m}$	1.85	2.42
	crystals with sector-like branches (P1b)	$40 < D_{max} < 2000\mu\text{m}$	1.97	2.02
	broad-branched crystals (Plc)	$10 < D_{max} < 100\mu\text{m}$	1.85	2.42
	broad-branched crystals (Plc)	$100 < D_{max} < 1000\mu\text{m}$	1.76	1.8
	stellar crystals with broad arms (P1d)	$10 < D_{max} < 90\mu\text{m}$	1.85	2.42
	stellar crystals with broad arms (P1d)	$90 < D_{max} < 1500\mu\text{m}$	1.63	1.67
	densely rimed dendrites (R2b)	$1800 < D_{max} < 4000\mu\text{m}$	1.76	2.3
	side planes (S1)	$300 < D_{max} < 2500\mu\text{m}$	1.88	2.3
	bullet rosettes, 5 branches at -42°C	$200 < D_{max} < 1000\mu\text{m}$	1.57	2.26
	aggregates of side planes	$600 < D_{max} < 4100\mu\text{m}$	1.88	2.2
	aggregates of side planes, columns & bullets (S3)	$800 < D_{max} < 4500\mu\text{m}$	1.88	2.1
	assemblies of planar polycrystals in cirrus clouds	$20 < D_{max} < 450\mu\text{m}$	1.88	2.45
	lump graupel (R4b)	$500 < D_{max} < 3000\mu\text{m}$	2	2.8
	hail	$5000 < D_{max} < 25000\mu\text{m}$	2	3
Simulations of Ice-Crystals shape				
	columns ($H=5*L$)	$100 < D_{max} < 1000\mu\text{m}$	1.86	2.53
	columns ($H=10*L$)	$100 < D_{max} < 1000\mu\text{m}$	1.87	2.44
	columns ($L=160\mu\text{m}$)	$100 < D_{max} < 1000\mu\text{m}$	1.06	1.04
	columns ($L = \sqrt{H}$)	$100 < D_{max} < 1000\mu\text{m}$	1.48	1.78
	thick star ($H = 0.2*L$)	$200 < D_{max} < 1200\mu\text{m}$	1.98	2.89
	thick star ($H = 0.1*L$)	$200 < D_{max} < 1200\mu\text{m}$	1.99	2.86
	thick stars ($H=40\mu\text{m}$)	$200 < D_{max} < 1200\mu\text{m}$	1.49	2.06
	thick stars ($H = \sqrt{L}$)	$200 < D_{max} < 1200\mu\text{m}$	1.76	2.48
	thin stars ($H=0.2*L$)	$100 < D_{max} < 1000\mu\text{m}$	1.96	2.89
	thin stars ($H=0.1*L$)	$100 < D_{max} < 1000\mu\text{m}$	1.94	2.75
	Thin stars ($H=40\mu\text{m}$)	$100 < D_{max} < 1000\mu\text{m}$	1.39	2.06
	thin stars ($H = \sqrt{L}$)	$100 < D_{max} < 1000\mu\text{m}$	1.74	2.51
	plates ($H= 0.2*L$)	$200 < D_{max} < 2000\mu\text{m}$	1.95	2.96
	plates ($H = 0.1*L$)	$200 < D_{max} < 2000\mu\text{m}$	1.92	2.91

	plates ($H=40\mu\text{m}$)	$200 < D_{max} < 2000\mu\text{m}$	1.65	2.03
	plates ($H = \sqrt{L}$)	$200 < D_{max} < 2000\mu\text{m}$	1.86	2.49
	rosettes ($L= 50\mu\text{m}$; $N_{max}=3$)	$50 < D_{max} < 500\mu\text{m}$	1.37	1.04
	rosettes ($L = \sqrt{H}$; $N_{max}=3$)	$50 < D_{max} < 500\mu\text{m}$	1.69	2.21
	rosettes ($L=100\mu\text{m}$; $N_{max}=4$)	$100 < D_{max} < 1000\mu\text{m}$	1.39	1.26
	rosettes ($L = \sqrt{H}$; $N_{max}=4$)	$100 < D_{max} < 1000\mu\text{m}$	1.65	2.16
	rosettes ($L=0.5H$; $N_{max}=5$)	$500 < D_{max} < 2000\mu\text{m}$	1.83	2.9
	rosettes ($L=0.25H$; $N_{max}=6$)	$500 < D_{max} < 2500\mu\text{m}$	1.78	2.97
	rosettes($L=100\mu\text{m}$; $N_{max}=6$)	$100 < D_{max} < 1000\mu\text{m}$	1.42	1.25
	rosettes($L = \sqrt{H}$; $N_{max}=6$)	$100 < D_{max} < 1000\mu\text{m}$	1.66	2.16
	capped columns (2 plates: $L_2=2.5L_1$; $H= L_1$)	$150 < D_{max} < 1400\mu\text{m}$	1.79	2.21
	capped columns (2 thick stars: $L_2=2.5L_1$; $H= L_1$)	$150 < D_{max} < 1400\mu\text{m}$	1.92	2.43
	$8 < N_{agg} < 30$ thick stars ($H = \sqrt{L}$) individual diameter of thick stars : $30 < L < 40\mu\text{m}$	$1000 < D_{max} < 4000$	1.79	1.92
	$8 < N_{agg} < 30$ plates ($H = 0.1*L$) individual diameter of plates : $20 < L < 30\mu\text{m}$	$600 < D_{max} < 2000$	1.8	1.81
	$8 < N_{agg} < 30$ plates ($H = \sqrt{L}$) individual diameter of plates : $20 < L < 30\mu\text{m}$	$600 < D_{max} < 2500$	1.59	1.69
	$2 < N_{agg} < 4$; columns ($L=160\mu\text{m}$) individual diameter of columns : $40 < H < 60$	$400 < D_{max} < 1500$	1.26	1.75
	$2 < N_{agg} < 4$; columns ($L = \sqrt{H}$) individual diameter of columns : $40 < H < 60$	$200 < D_{max} < 1000$	1.45	2.07
	$2 < N_{agg} < 4$; thick stars ($H= 0.2*L$) individual diameter of thick stars : $40 < L < 60\mu\text{m}$	$400 < D_{max} < 3000$	1.82	2.62
	$2 < N_{agg} < 4$; thick stars ($H= 0.1*L$) individual diameter of thick stars: $40 < L < 60\mu\text{m}$	$400 < D_{max} < 3000$	1.63	2.62
	$2 < N_{agg} < 4$; thick stars ($H= 40\mu\text{m}$) individual diameter of thick stars: $40 < L < 60\mu\text{m}$	$400 < D_{max} < 3000$	1.87	2.25
	$2 < N_{agg} < 4$; thick stars ($H = \sqrt{L}$) individual diameter of thick stars: $40 < L < 60\mu\text{m}$	$400 < D_{max} < 3000$	1.72	2.46
	$2 < N_{agg} < 4$; thin stars ($H= 0.2*L$) individual diameter of thin stars: $30 < L < 60\mu\text{m}$	$300 < D_{max} < 2000$	1.64	2.52
	$2 < N_{agg} < 4$; thin stars ($H= 0.1*L$) individual diameter of thin stars: $30 < L < 50\mu\text{m}$	$300 < D_{max} < 1500$	1.72	2.52
	$2 < N_{agg} < 4$; thin stars ($H= 40\mu\text{m}$) individual diameter of thin stars: $30 < L < 50\mu\text{m}$	$300 < D_{max} < 1500$	1.46	2.14
	$2 < N_{agg} < 4$; thin stars ($H = \sqrt{L}$) individual diameter of thin stars: $30 < L < 50\mu\text{m}$	$300 < D_{max} < 2000$	1.53	2.37
	$2 < N_{agg} < 4$; plates ($H= 0.2*L$) individual diameter of plates : $30 < L < 50\mu\text{m}$	$300 < D_{max} < 2000$	1.87	2.57
	$2 < N_{agg} < 4$; plates ($H= 0.1*L$) individual diameter of plates : $30 < L < 50\mu\text{m}$	$250 < D_{max} < 1500$	1.61	2.37
	$2 < N_{agg} < 4$; plates ($H= 40\mu\text{m}$) individual diameter of plates : $30 < L < 50\mu\text{m}$	$250 < D_{max} < 1500$	1.64	1.99
	$2 < N_{agg} < 4$; plates ($H = \sqrt{L}$) individual diameter of plates : $30 < L < 60\mu\text{m}$	$250 < D_{max} < 1500$	1.76	2.29
	$3 < N_{agg} < 20$; spheres individual diameter of spheres : $D = 60\mu\text{m}$;	$300 < D_{max} < 2000\mu\text{m}$	1.45	1.74
	$3 < N_{agg} < 50$; spheres individual diameter of spheres : $D = 150\mu\text{m}$;	$100 < D_{max} < 1000\mu\text{m}$	1.54	1.84

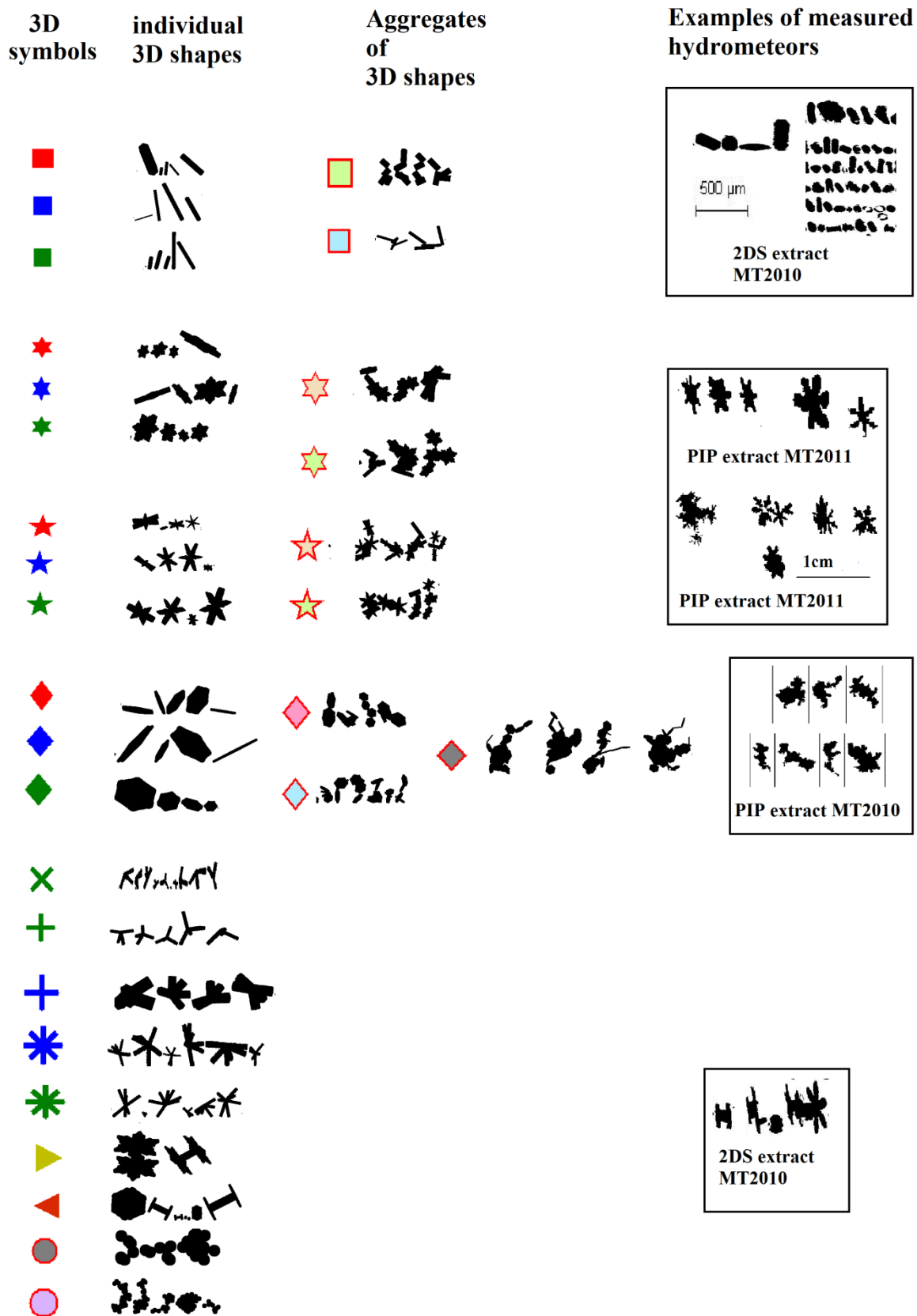


Figure 4 : On the left column are presented examples of 2D projections of randomly oriented 3D shapes of single hydrometeors with their corresponding symbols as they are represented in figure 7 and in table 4. In the middle column, examples of aggregates composed of single individual shapes as shown in the left column. The right column shows examples of crystals resembling what has been recorded in different aircraft measurement campaigns.

For each random orientation, it is possible to calculate a density. How do those density values compare to those determined by your mass dimensional relationships?

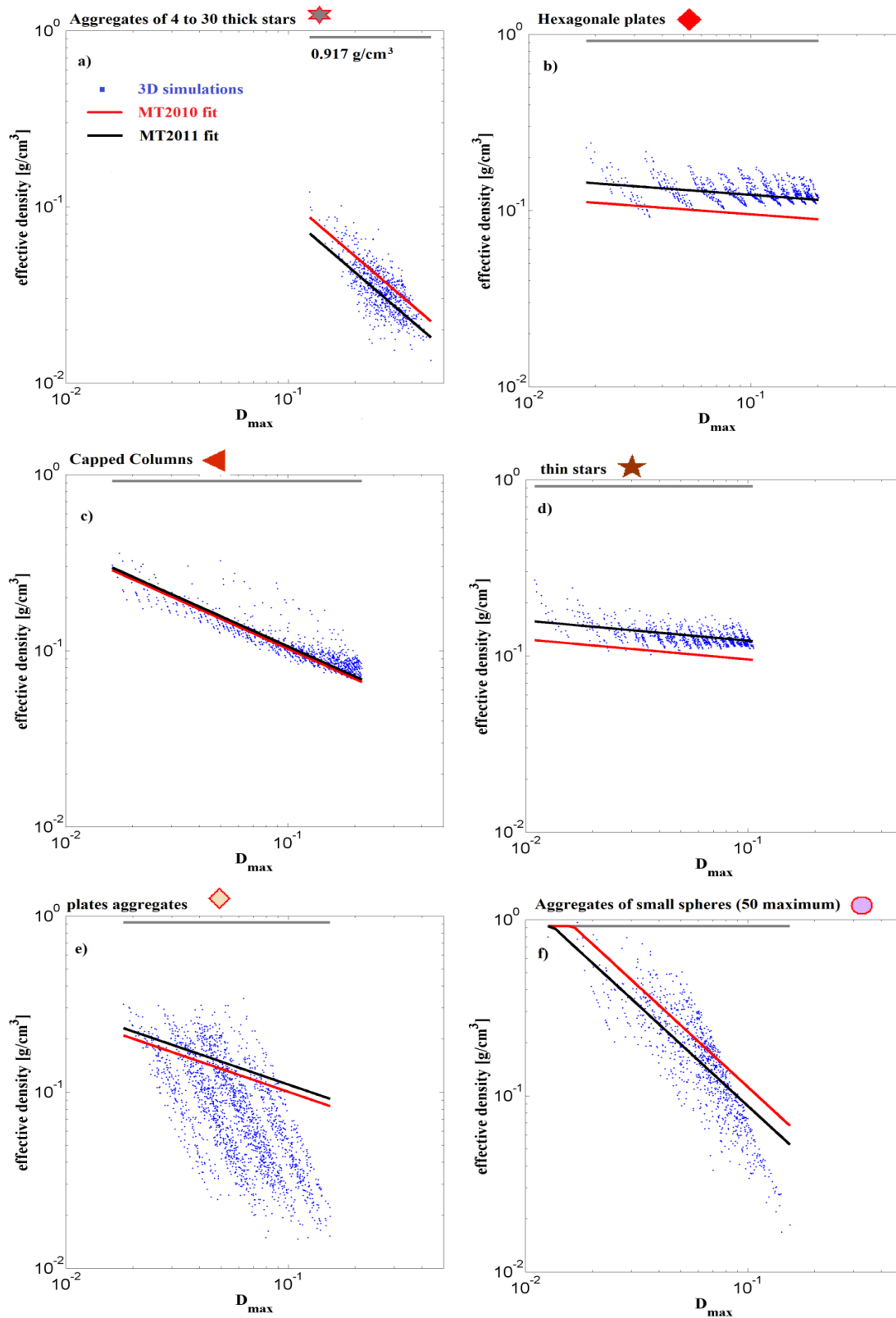


Figure 5 : Blue dots show effective density calculated from 3D simulations, which are compared with linear fits of $\ln(\alpha)$ as a function of β , found for MT2010 (red line) and MT2011 (black line).

4. Using the alpha and beta values given in the summary for the mass dimensional relationship, I get $m=0.0244 \cdot D^{2.44}$ or $m=0.0266 \cdot D^{2.44}$. This is really heavy for large particles, and substantially different for published mass dimensional relationships. The authors need to explain why there is such a substantial difference. Is it specifically related to your dataset? Or, are all of the others wrong, and if so, why?

Mass-diameter relationships are calculated in this study with the help of measured reflectivity at 94GHz. Subsequently CWC can be calculated from PSD and $m(D)$. Most recently the international HAIC-HIWC campaign which took place during January- March 2014 out of Darwin allowed to confront the radar reflectivities of the RASTA radar and the direct measurements of the IWC using the IKP (isokinetic evaporator probe). This confrontation allowed to improve the method correcting the radar reflectivity close to the aircraft within 900m below and above the aircraft.

We integrated into our answers to the reviewers and in the new version of the radar RASTA data these results taking into account the corrections of the reflectivity of RASTA in the vicinity of the aircraft.

With the corrected new dataset of radar reflectivities we have then recalculated the mean m - D coefficients. For example if the 2DS is solely used to calculate σ of the S - D power law, and then calculate the m - D exponent β and constrain α , we find for:

$$MT2010: m(D_{\max}) = 0.0098 \cdot D_{\max}^{2.26}$$

$$MT2011: m(D_{\max}) = 0.0082 \cdot D_{\max}^{2.22}$$

And when σ is calculated from the 2DS plus the PIP images we receive :

$$MT2010: m(D_{\max}) = 0.0093 \cdot D_{\max}^{2.25}$$

$$MT2011: m(D_{\max}) = 0.0057 \cdot D_{\max}^{2.06}$$

These mean values of m - D relationships are presented in the revised manuscript and are compared with other m - D relationships in the new manuscript.

Further comments:

Page 2984 line 2: Ice hydrometeors (without the word “ice” you could be talking about rain as well).

“In this study the density of ice hydrometeors in tropical clouds is derived from a combined analysis of particle images of 2-D array probes...”

Page 2987 lines 9-12: Relationships derived in SH2010 were derived numerically, and tested with aircraft data. (See major point #1 above).

Page 2987 line 13: There should be a period at the end of this line.

“Schmitt and Heymsfield (2010, hereafter SH2010) have simulated the aggregation of plates and columns. Fractal 2D and 3D analyses calculated from the box counting method (Tang and Marangoni 2006) stated that the fractal coefficient in the 3D space is equal to β . This allowed to derive a relationship that calculates the exponent β from the 2D fractal dimension of the 2D images. Once β has been fixed, the pre-factor α is calculated from the area measurement.”

Heymsfield et al. (2010, hereafter H10) demonstrate that a strong relationship exists between α and β coefficients and argue that the BF95 relationship overestimates the prefactor a for stratiform clouds, whereas a is underestimated for convective clouds. “

Page 2988 line 21: Was the Nevzorov probe used a standard version or modified with a deeper groove? The standard version likely underestimates CWC when there are high concentrations of larger particles which can shatter and partially bounce out on impact. (See Korolev's 2011 BAMS article)

Yes we use the deep cone version of the Nevzorov.

Page 2990 line 8: TSD is not defined. Could you mean AsD?

“Examples of PSD and AsD are presented in Fig. 1...”

Page 2990 line 24: How do the measured aspect ratio values from the probe measurements compare to the average aspect ratio calculated for the theoretical particles (in the appendix)? (Densities as well)

Average aspect ratio of theoretical simulations may not be entirely comparable with experimentally measured average As due to possible orientation of crystals. In case that crystals are sampled randomly oriented on the aircraft, simulations and observations of As are fully comparable.

Page 2991 line 24: You assume that the reflectivity at the aircraft is the value linearly interpolated between the value 300m above and the value 300m below. How different are these values typically? Difference and standard deviation and how much uncertainty does this cause in the results? It might be interesting to look at the difference between 300 and 900 meters above and see if that difference is similar to the difference between 300 above and 300 below.

Reflectivity differences between the Nadir antenna and Zenith antenna 300 m above and 300 m below the aircraft are of the same order than the differences between 300 and 900 meters above and also below. These differences are in the range of about [1.6 - 3.5dBZ], with an exception for the flight 49 of MT2011. Clouds in this flight were very small isolated convective flight and were not taking into account to calculate the mean mass-diameters coefficients.

A linear interpolation of measured reflectivities below and/or beyond the aircraft in order to estimate the reflectivity at the aircraft flight altitude, would result in a maximum uncertainty of the estimated reflectivity at flight level of 2dBZ, which means a maximum error of 20% on the retrieved CWC.

Table 2: Mean difference in dBZ and standard deviation of RASTA reflectivities calculated between two radar gates having a distance of 600 meters.

Flight	$Z_{Zenith}(300)-Z_{Zenith}(900m)$		$Z_{Nadir}(300m)-Z_{Nadir}(900m)$		$Z_{Nadir}(300m)-Z_{Zenith}(300m)$	
	Mean [dBZ]	Std [dBZ]	Mean [dBZ]	Std [dBZ]	Mean [dBZ]	Std [dBZ]
15	3.16	2.82	3.45	4.03	3.22	3.33
17	2.94	2.81	3.00	3.06	2.56	2.59
18	2.07	2.43	2.49	2.75	1.59	2.13
19	4.33	3.82	2.98	3.51	3.46	3.52
20	2.68	2.50	2.66	2.55	1.6	1.68
45	4.24	4.01	3.69	3.93	3.33	3.28
46	4.98	4.39	3.76	3.94	3.36	3.58
49	6.43	5.41	7.34	6.77	5.11	5.69
50	4.56	6.11	4.81	6.49	2.10	5.69

Page 2992 & figure 4: Doesn't 5 g/m³ CWC seem rather high? Your dBZ values are very high. My concern is that the Protat 2007 parameterization appears to include data only up to about 10dBZ. Could higher values be influenced by graupel or hail? This should show up in the PIP data.

We do not understand why you refer the 5g/m³ to the Protat 2007 parametrisation, knowing that the Protat parameterization was not used to calculate the retrieved CWC used in this study.

However, as we can see in figure 6, during the high IWC (5g/m³), 2D images recorded by the PIP show few graupels with a size around 1mm to 2mm.

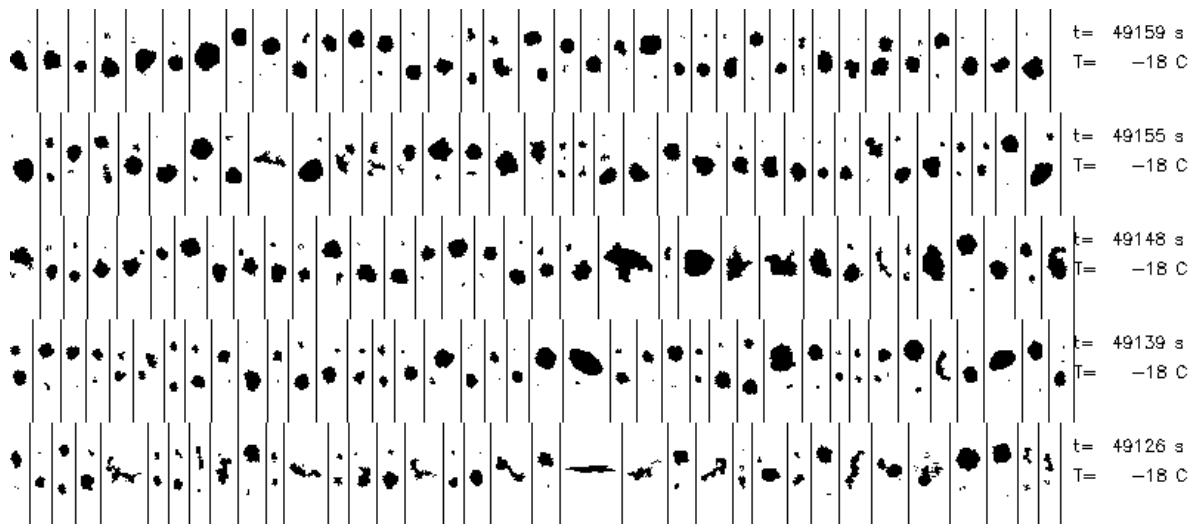


Figure 6: Extract of PIP image catalogue of flight 18. Bars between 2 particles constitute 7mm in length.

Figure 4 should also have the dBZ value derived for the pass.

We do not understand the question.

Page 2994 line 13: Suggest that you try the Schmitt and Heymsfield method for calculating alpha directly from the particle area data and compare to your results.

Implementing the Schmitt and Heymsfield method is beyond the scope of this study. We are not sure of having all the details to implement and run the method.

Page 2995: Sigma for each particle shape is calculated, but it is unclear how.

The σ is calculated for the entire population of crystals imaged during 5 seconds with 2D-S plus PIP probes. The method is explained above in answering to your comment 2 in the beginning.

Is the area and maximum dimension determined for each random orientation, then a fit done to maximum dimension versus area for all of the individual rotations? If so, then your sigma value may be more related to the orientation rather than the size to area relationship.

Each 3D crystal shape includes 1000 simulations where the crystal size and orientation varied in the 3D space. There is only one power fit for $m(D_{max})$ and $S(D_{max})$ per single 3D crystal shape (including size and orientation variation) (see also answer to the comment 2 and figure 1 and Appendix A on the current version of the paper).

Of course the $m(D_{max})$ and $S(D_{max})$ are related to the 3D orientation, however, also D_{max} is dependent on the 3D orientation.

Page 2995 line 21-22: using 1.0 for sigma yields a value of 0.6 for beta (outside the range presented on line 21).

*Taken into account the added simulations and orientations uncertainties now we have:
 $\beta = 1.93 \cdot \sigma - 1.02$ (equation 11 in the current version), with σ in the range [1.05 ; 2].*

Page 2995: How many of your theoretical particles are truly irregular? How many of your observed particles are truly irregular?

See new version of figure 6 in the answer to the comment 3.

Page 2997, line 17: Consider comparing either Brown and Francis and/or Heymsfield et al 2004. There are no assumptions on shapes in these as well.

An extended study on the impact of the variability of $m(D)$ coefficients on CWC and CWC-Z, including Brown & Francis has been added in the revised version of the manuscript; see also answer to the second reviewer for all the details.

Page 2998 line 25: From here, there is a lot of discussion of the basic properties of the clouds measured during the campaigns. It isn't clear why it is important to discuss this now. Much of it isn't relevant to the study.

This part has been removed in order to take into account, the comments of referee #2 and #3.

Page 3001 line 3: It would be interesting to plot some typical density values from your alpha beta pairs as compared to density values from the literature.

Averaged values of $m(D)$ coefficients found for MT2010 and MT2011 with σ determined from 2DS only are relatively close. They give less mass for a same D_{max} if they are compared with $m(D)$ coefficients of H2010 for NAMMA. Average values for $m(D)$ coefficients when 2DS plus PIP are used to determine σ , show similar trends between H2010 for cloud convectively generated and MT2011. $m(D)$ coefficients given by Mitchell 1996 give less mass for a same D_{max} compared with the $m(D)$ relationships cited before, with an exception for the lump graupel's $m(D)$ coefficients which give largest mass for particles beyond 1mm compared to all the other $m(D)$ relationships. Mitchell's lump graupel still give larger mass for particles beyond 500 μ m compared to MT2010 and MT2010 $m(D)$ from T-matrix and H2010 convectively generated $m(D)$.

Note that for MT2010 when using the 2DS plus PIP to determine σ we find $m(D)$ coefficients close to those found with 2DS with $\alpha=0.0093$ and $\beta=2.25$

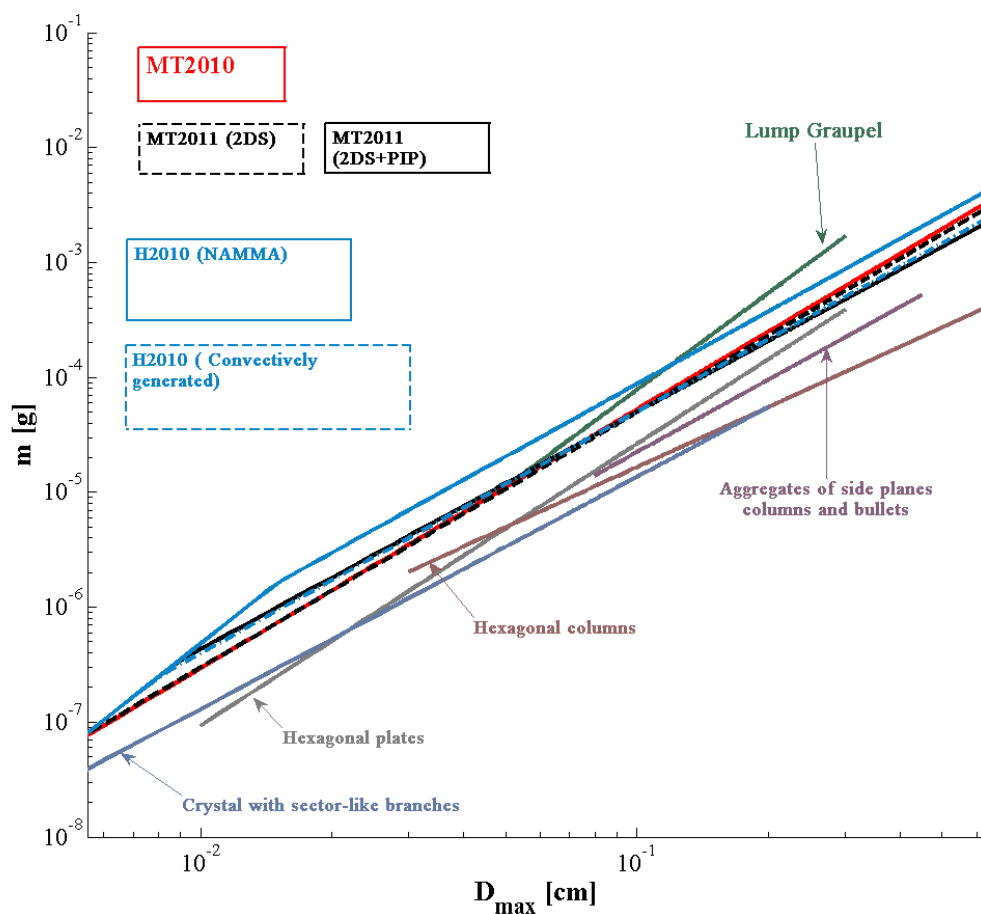


Figure 7 : Mass of ice crystals in gram on y axis, as a function of their D_{max} in cm on the x axis. The red line represents mean values of $m(D)$ coefficients for MT2010 when σ is determined from 2D-S plus PIP images with $\alpha=0.0098$ and $\beta=2.26$. Likewise, the black dashed line represents $m(D)$ coefficients for MT2011 with $\alpha=0.0057$ and $\beta=2.06$. The black line represents MT2011 when σ is determined from 2DS only with $\alpha=0.0082$ and $\beta=2.22$. The blue line represents $m(D)$ coefficients taken from H2010 for the NAMMA campaign with $\alpha=0.011$ and $\beta=2.1$. Dashed blue line stands for H2010, but for convectively generated systems with $\alpha=0.0063$ and $\beta=2.1$. Blue grey line is given by Mitchell 1996 for crystal with sector-like branches with $\alpha=0.00142$ and $\beta=2.02$. Grey line (Mitchell 1996) represents hexagonal plates with $\alpha=0.00739$ and $\beta=2.45$. Brown grey line (Mitchell 1996) represents hexagonal columns with $\alpha=0.000907$ and $\beta=1.74$. Purple grey line (Mitchell 1996) is for aggregates of side planes columns and bullets with $\alpha=0.0028$ and $\beta=2.1$. Green line (Mitchell 1996) is for Lump Graupel with $\alpha=0.049$ and $\beta=2.8$.

Given the extremely high dBZ values recorded, can these results be generalized?

Results presented in this study have been compared to other methods of $m(D)$ estimations. Details are given in the answer to reviewer nr.2 and in the revised version of the manuscript. The variability of $m(D)$ coefficients from T-matrix retrievals as a function of the temperature is similar to the one presented by SH2010 (more details in answer to comments of Referee 1 and 2),

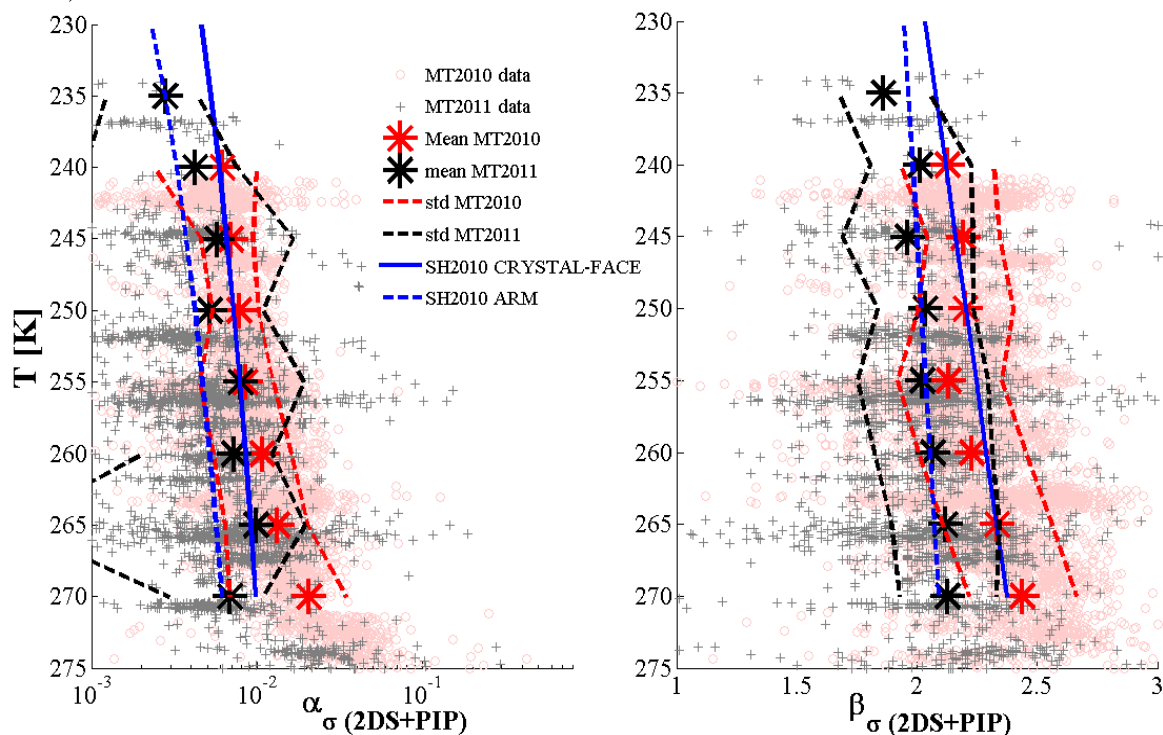


Figure 8 : Vertical profile of $m(D)$ coefficients constrained by T-matrix and the variability of S-D exponent σ calculated from 2D-S plus PIP images. (a) α_σ versus the temperature in K. (b) β_σ versus the temperature in K. Pink circle show data points (5-seconds time step) of MT2010, grey crosses show MT2011 data. Red and black stars present mean values of $m(D)$ coefficients in 5K temperature intervals for MT2010 and MT2011, respectively. Dashed red and black lines show standard deviations of MT2010 and MT2011, respectively, from the mean value. Blue solid and dashed lines show vertical profiles of SH2010 obtained for CRYSTAL-FACE, and for ARM, respectively.

Page 3004 line 4-5: When I compare these alpha and beta pairs to BF, the results show a similar density predicted for 200 micron particles, then for larger (3000 um) up to a factor of 5 higher density for your results. This difference (with BF and others) needs to be shown and explained.

Brown and Francis relationships were calculated for $D=(Lx+Ly)/2$, where Ly is the size along the array diode and Lx the size perpendicular to Ly , whereas D_{max} is the size of the circle which englobes the entire 2D image. Therefore, due to discrepancies in diameter definition, BF seems not appropriate to be compared on a same plot with mass versus D_{max} .

Page 3006 line 9: It would be good to show typical plots of the shape of the PSDs so that they can be compared to other data. Gamma fit parameters (λ , μ , N_0) as are commonly shown would be helpful.

PSD cannot be easily fitted with Gamma distributions, the concentration of small ice hydrometeors would be badly represented. Start fitting the PSD would end in adding a

somewhat different topic to that manuscript. The idea should be followed up, preparing a separate study on fitting of PSD for available data sets.